An Investigation on Mathematical Models of Wire Rope Isolators

Conference Paper · December 2006

2 authors, including:

Feng Tyan
Tamkang University
51 PUBLICATIONS **555** CITATIONS

SEE PROFILE

中華民國力學學會第三十屆全國力學會議 彰化縣大葉大學機械與自動化工程學系 95 年 12 月 15-16 日
The 30thNational Conference on Theoretical and Applied Mechanics, December 15-16, 2006, DYU, Changhwa, Taiwan, R.O.C.

An Investigation on Mathematical Models of Wire Rope Isolators

Feng Tyan
Computational Dynamics and Control Lab
Dept. of Aerospace Engineering
Tamkang University
Tamshui, Taipei County, Taiwan 25147, R. O. C.

Shun-Hsu Tu and **Jeffrey Wu**
Mechanical and Systems Research Laboratories
Industrial Technology Research Institute,
Chu Tung, Hsin Chu, Taiwan 310, R. O. C.

ITRI Project: 3000108944

***Abstract*— Vibration isolation systems using helical wire rope isolators are known to be highly effective in controlling both shock and vibration and have been used in numerous space and military applications. For damping response, the force-displacement relationship of a wire rope isolator is highly nonlinear and history-dependent. For satisfactory analysis of such behavior, it is important to be able to characterize and to model the phenomenon of hysteresis accurately. Both Tinker and Bouc-Wen models that had been proposed for response studies of wire rope isolators are examined in this paper. For helical type wire-rope isolator Bouc-Wen's model, compared with Tinker's model, predicts much more intimate behavior as observed in experiment datum.**

keywords: **wire rope, Tinker model, Bouc-Wen model, hysteresis loop.**

I. Introduction

Wire rope isolators are simple devices made of stainless steel stranded cable and retaining bars. They provide a high performance level of shock and vibration isolation. They are not affected by temperature and are environmentally stable, hence have been used in numerous space and military applications.

The structure of typical wire rope isolators can be described by the followings [1]:

1) comprised of stainless steel stranded cable,
2) threaded through aluminum alloy retaining bars,
3) crimped and mounted for effective vibration isolation.

Figures 1 and 2 illustrate some typical commercially available types of wire rope isolators.

Fig. 1. Typical Wire Rope Isolators

Fig. 2. Circular Arch Isolator

We use a helical wire rope isolator as an example to further illustrate its configuration. As we have mentioned previously, a wire rope, or cable, typically consists of several strands of wire wrapped around a metallic or fibrous core, by winding the cable in the form of a helix and fastening it with clamps to maintain the shape, helical isolators are constructed, see Figure 3. These helical devices can then be arranged as desired to form a vibration isolation system. An example system configuration is shown Figure 4.

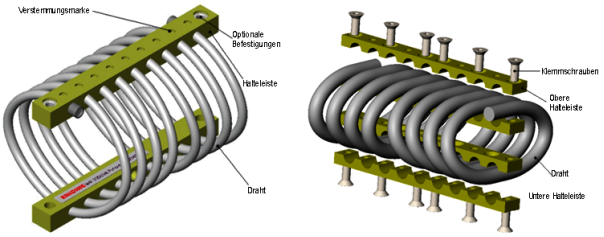

Fig. 3. Helical Wire Rope detail configuration

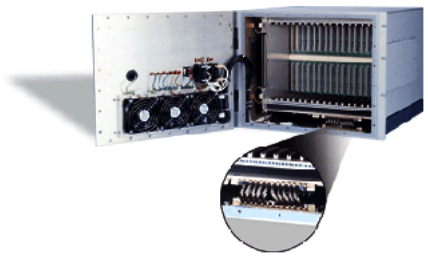

Fig. 4. An electrical cabinet using wire rope isolation system

The main principle by which wire rope systems are designed and by which they work are inherent interfacial damping, or sliding friction, and adjacent wires move relative to each other, friction causes part of the kinematic energy of the wires to be converted into heat, thereby dissipating vibrational energy. Quantitatively, the damping characteristics of helical isolators depend on the following factors [1]:

1) the cable diameter R_c, R_h,
2) number of strands,
3) number of loops per isolator,
4) lay angle of the strands α,
5) the overall dimensions of the isolator,

See Figure 5([2]), for the structure of a typical wire rope and definitions of the variables used above.

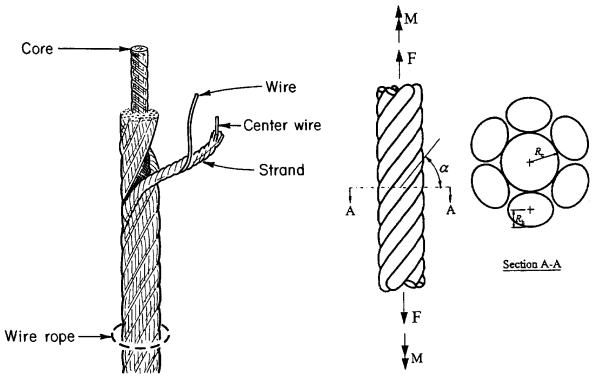

Fig. 5. Structural elements in a typical wire rope

Since wire rope isolators are made of stainless steel stranded cable, they have significant advantages over conventional rubber or elastomeric isolators for the severe operational environments of mechanical systems. In summary, they perform well through a wider range of temperatures ($-400°$F to $700°$F), and are less susceptible to wear and deterioration than elastomers, and are able to provide isolation in all directions (see Figure 6).

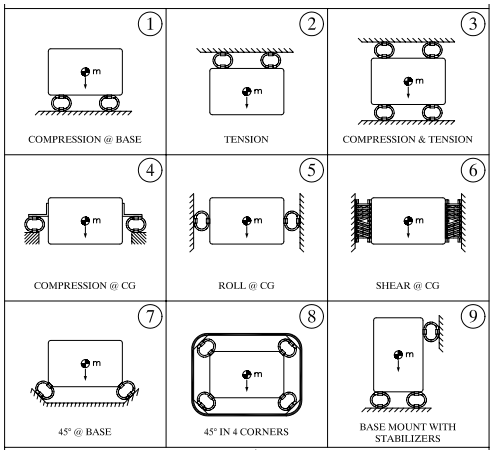

Fig. 6. Mounting Configurations

A good isolator system has two components, a spring to support the load and a damping element to dissipate the input energy. Wire rope isolators possess both of the above properties. In addition, owing to the capability of working under severe environment, wire Ropes are suitable for a broad range of applications. They are ideal for applications such as

1) Cases for electronic equipment,
2) Mobile electronic equipment [3] (See e.g. Figure 7),
3) Chemical machines, Medical equipment,
4) Pump, Generator and Compressor Isolation,
5) Transportation of sensitive equipment, or shipping containers and skids to eliminate damage caused by shock and vibration to equipment during transport, see Figure 8.

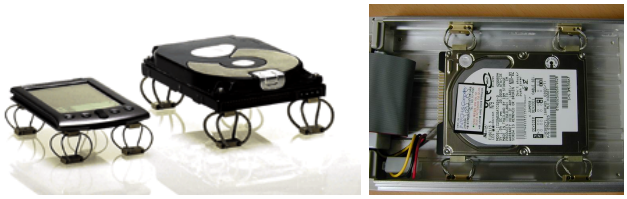

Fig. 7. Wire rope isolator used in a PDA and hard disk drive

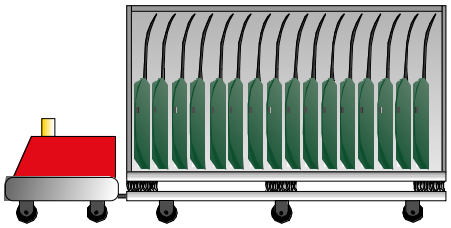

Fig. 8. Wire rope isolator used in shipping door panels

The major feature of the nonlinear restoring force of wire rope isolator is its hysteretic characteristic (See Figure 9), i.e., it depends not only on the instantaneous deformation but also on the past history of deformation. In this paper, the mathematical modelling of the dynamic behavior of a wire rope vibration isolator is investigated. Two kinds of mathematical model will be considered, namely,

1) Tinker's model,
2) Bouc-Wen's model.

II. Tinker's Model

Several nonlinear one-dimensional mathematical models proposed by Tinker will be investigated in an effort to model the frequency response and damping characteristics of the wire rope isolator model shown in Figure 10 [1].

The Tinker's model is described by a second-order differential equation and can be divided into the following categories:

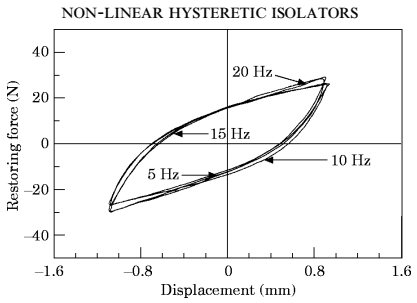

Fig. 9. Hysteresis curves from test

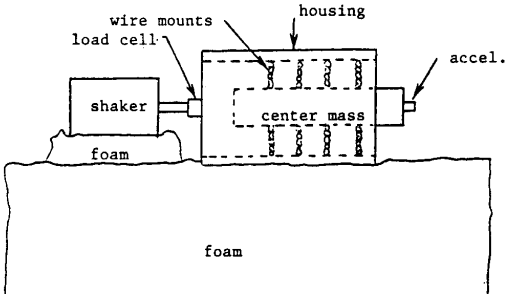

Fig. 10. Test Setup for Tinker's Model

1) Nonlinear Stiffness and Simple Linear Damping - No Hysteresis

$$m\ddot{x} + c[\dot{x} - \dot{x}_s] + k[x - x_s \pm \varepsilon^2(x - x_s)^3] = 0.$$

where

c: is the viscous damping coefficient,
k: is the stiffness,
ε^2: nonlinear spring constant,
x: is the absolute displacement of the center of mass to the shaker,
x_s: is the absolute displacement of the shaker.

2) Nonlinear Stiffness and Coulomb Friction - No Hysteresis

$$m\ddot{x} + f\text{sgn}(\dot{x} - \dot{x}_s) + k[x - x_s \pm \varepsilon^2(x - x_s)^3] = 0.$$

where

f is the Coulomb friction force.

3) n^{th}-Power Velocity Damping- Hysteresis Added

$$m\ddot{x}+c|(\dot{x}-\dot{x}_s)^n|\text{sgn}(\dot{x}-\dot{x}_s)+k[x-x_s\pm\varepsilon^2(x-x_s)^3] = 0,$$

where

c is the velocity damping coefficient

and

$n = 0$ - Coulomb damping,
$n = 1$ - Viscous damping,
$n \geq 2$ - hysteresis.

4) n^{th}-Power Velocity Damping + Variable Coulomb Friction

$$m\ddot{x} + k[x - x_s \pm \varepsilon^2(x - x_s)^3] + \left\{c|(\dot{x} - \dot{x}_s)^n| + f[1 - a(x - x_s)^2]\right\}\text{sgn}(\dot{x} - \dot{x}_s) = 0.$$

5) n^{th}-Power Velocity Damping + Variable Coulomb Friction + Modifications - Hysteresis Added with Modification

$$m\ddot{x} + r\left\{k[x - x_s \pm \varepsilon^2(x - x_s)^3] + b\right\} + \left\{c_n|(\dot{x} - \dot{x}_s)^n| + f[1 - a(x - x_s)^2]\right\}\text{sgn}(\dot{x} - \dot{x}_s) = 0, \quad (2.1)$$

where

b: the distance each hysteresis backbone curve lies above the origin,
r: stiffness parameter, to account for the reality that dynamic stiffness curves do not necessarily pass through the centers of corresponding hysteresis curves.

Figure 11 demonstrates the contributions to the model from viscous and Coulomb damping forces.

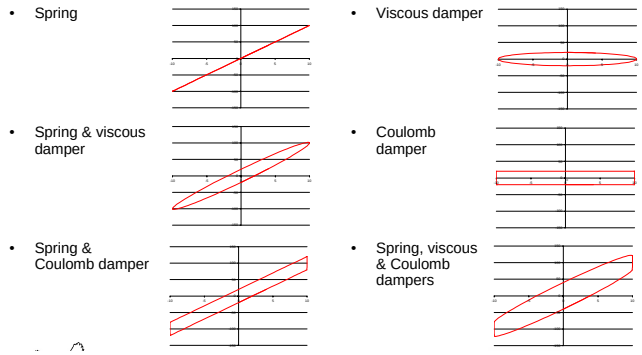

Fig. 11. Linear spring with viscous and Coulomb damper

Example 2.1: The following typical values of data for Tinker's model (2.1) are taken from [1]. The hysteresis curves for different parameters are illustrated in Figures 12-13. In Figure 12, the damping coefficients are changed to see its effects. As we can tell from these figures, in the steady state, when c increases, the "size" of the hysteresis loop shrinks, and the loop becomes rounder. While for the case of changing spring stiffness k, from Figure 13, it is easy to identify that the slope of the hysteresis loop increases with the increasing of k.

TABLE I
PARAMETERS USED FOR EXAMPLE 2.1

parameters	value
mass	$m = 0.225817$ (lb)
spring stiffness	$k = 168$
dampting ratio	$\zeta = 0, 0.25, 0.5, 0.75$
nonlinear spring constant	$\varepsilon^2 = 1043$
bias	$b = 0$ (lb)
Coulomb friction	$f = 0.2678$ (lb)
damping exponent	$n = 2$
frequency	$\omega = 60 \cdot 2\pi$ (rad/sec)

III. BOUC-WEN MODEL

We adopt a single-degree-of-freedom model (Figure 14) that has nonlinear stiffness and various damping mecha-

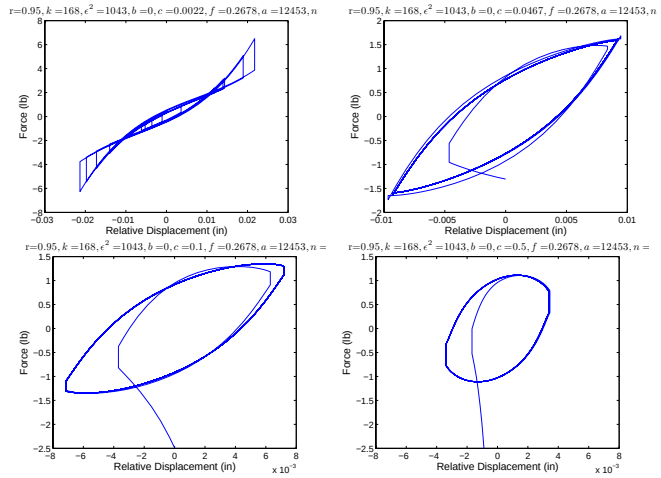

Fig. 12. Hysteresis Curves for $\omega = 60 \cdot 2\pi$(rad/sec), $u_0 = 0.0125$in and various c

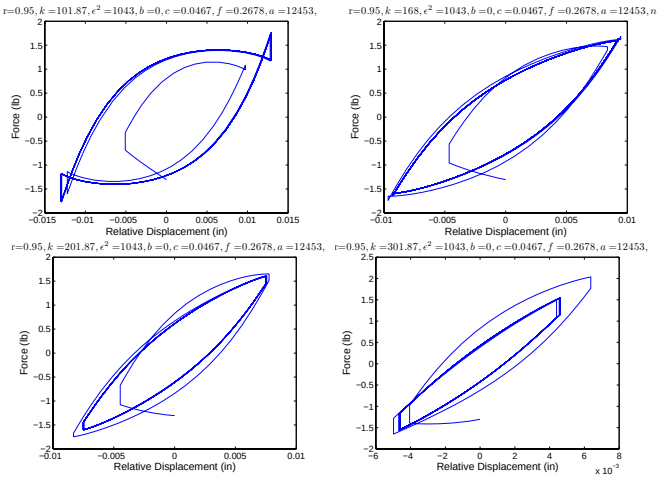

Fig. 13. Hysteresis Curves for $\omega = 60 \cdot 2\pi$(rad/sec), $u_0 = 0.0125$in and various k

nisms, including linear viscous damping, constant Coulomb friction, nth-power velocity damping, and combined nth-power and variable Coulomb friction damping,

$$m\ddot{x}(t) + F_r(t) = F(t), \tag{3.1}$$

where $F_r(t)$ is the restoring force

$$F_r(t) \triangleq kx(t) + c\dot{x}(t) + r[x(t), \dot{x}(t)], \tag{3.2}$$

and

m: the mass of the isolator,
$x(t)$: the absolute displacement of isolator,
$F(t)$: external excitation,
$r[x(t), \dot{x}(t)]$: hysteretic restoring force.

Elastic element of cable wire assembly exhibit hysteretic nonlinearity. It is found, however, the restoring force can be expressed as the sum of "nonlinear non-hysteretic" force and "pure hysteretic" force. In the actual system it is difficult to describe the damping force exactly due to its complicated

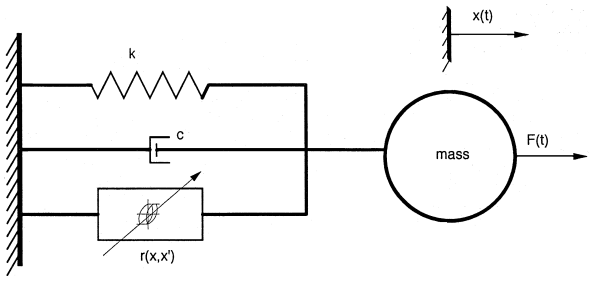

Fig. 14. SDOF Math Model

nature. A new parameter is proposed to describe the character between linear and dry friction damping. Owing to this new parameter, the order of the differential equation becomes three instead of two. The result of parameter identification shows this model can express hysteretic character effectively.

A. Standard Bouc-Wen Model

A standard Bouc-Wen model describing the hysteresis restoring force can be found in, e.g. [4, 5], it is expressed as

$$F_r(t) = kx(t) + c\dot{x}(t) + dx^3(t) + z(t), \tag{3.3}$$

where

$x(t)$ is the absolute displacement of isolator,
$z(t)$ is the hysteretic auxiliary variable.

The hysteretic auxiliary variable is governed by the following differential equation

$$\dot{z}(t) = \dot{x}(t)\left\{\alpha - |z(t)|^n\left[\gamma + \beta \cdot \mathrm{sgn}(\dot{x})\mathrm{sgn}(z)\right]\right\}, \tag{3.4}$$

where α, β, γ and n are the "loop parameters" to be calibrated from experimental tests which control the shape and the magnitude of the loop [5]. The hysteretic variable $z(t)$ has a finite ultimate value z_m which corresponds to the displacement x_m, that is

$$z_m = \left[\frac{\alpha}{\beta + \gamma}\right]^{\frac{1}{n}}. \tag{3.5}$$

Two cases can be considered here:

1) $\dot{x}(t) > 0$ (loading),
   a) $\beta + \gamma > 0$: softening stiffness,
   b) $\beta + \gamma = 0$: quasi-linear stiffness,
   c) $\beta + \gamma < 0$: hardening stiffness.
2) $\dot{x}(t) < 0$ (unloading),
   a) $\beta - \gamma > 0$: softening stiffness,
   b) $\beta - \gamma = 0$: quasi-linear stiffness,
   c) $\beta - \gamma < 0$: hardening stiffness.

Figure 15 illustrates the effects of β and γ in Bouc-Wen model.

Example 3.1: Consider the following parameters shown in Table II for the stand Bouc-Wen model. The hysteresis curves are shown in Figure 16. From these curves we know that larger damping coefficient c widens the hysteresis loop.

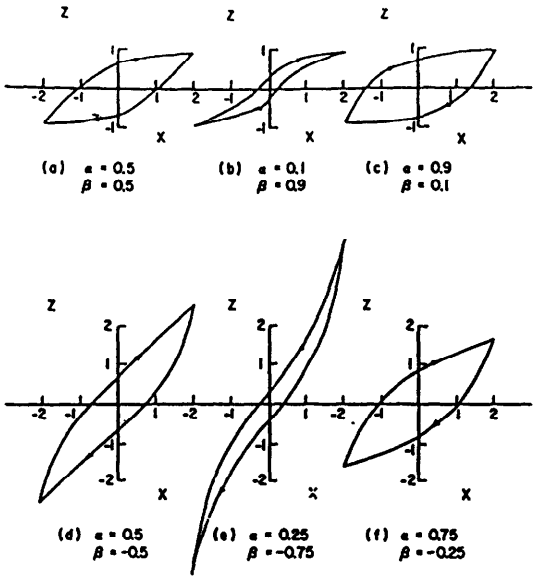

Fig. 15. Effects of β and γ in Bouc-Wen model

TABLE II

PARAMETERS FOR EXAMPLE 3.1

parameter	value
mass	$m = 0.5$(kg)
spring constant	$k = 100$
damping coefficient	$c = 0.8, 2.0, 20$
B-W model parameters	$\alpha = 34.422$
	$\beta = 8.94$
	$\gamma = -1.5$
	$n = 0.553$

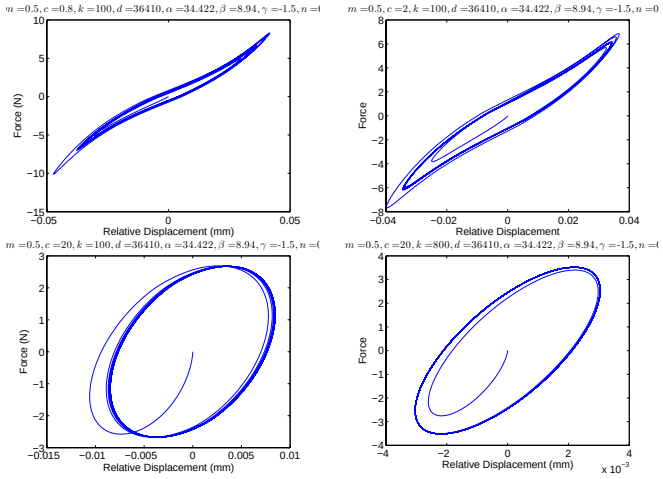

Fig. 16. Standard Bouc-Wen model, (a) $c = 0.8, k = 100$, (b) $c = 2.0, k = 100$, (c) $c = 20, k = 100$, (d) $c = 20, k = 800$

B. Symmetric Soft-Hardening Hysteresis Model

For a helical isolator, in the case of no preloading and under cyclic loading, the experimental hysteresis loops in both shear and roll modes (Figure 17) are symmetric due to symmetric configuration of the isolator [6, 7]. It is seen that the isolator displays softening hysteresis loops in relatively small deformations. However, when the deformation of the isolator reaches a certain level, the stiffening of hysteresis loops occurs (see Figure 18). This feature is referred to as soft-hardening hysteresis.

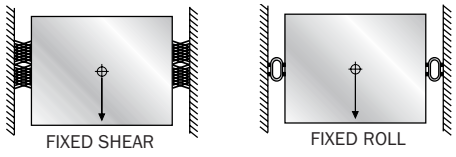

Fig. 17. The shear model and roll mode of helical isolator

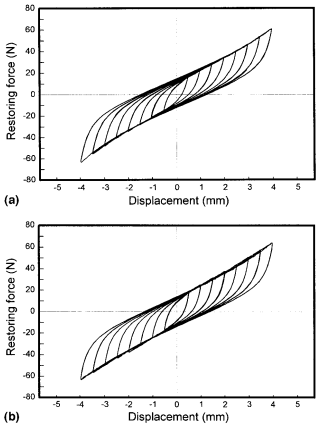

Fig. 18. Experimental hysteresis loops: (a) Shear mode, (b) Roll mode

For a soft-hardening hysteretic system, the restoring force can be modelled as the following [6]:

$$F_r(t) = F_{1s}(t)F_{2s}(t), \tag{3.6}$$

where

$$F_{1s}(t) \triangleq 1 + k_2 x^2(t) + k_3 \ \text{sgn}(x)x^3(t), \tag{3.7}$$

$$F_{2s}(t) \triangleq kx(t) + z(t), \tag{3.8}$$

Example 3.2: Consider the hysteresis Loop for Cyclic Loading: Shear/Roll mode. The related parameters are chosen as the followings:

$$k = 9.225, k_2 = 0.017, k_3 = -0.001,$$
$$n = 0.553, \alpha = 31.262, \beta = 9.726, \gamma = 2.155.$$

The corresponding hysteresis curves are shown in Figure 19, which shape is apparently symmetric.

C. Asymmetric Hysteresis Model

When the helical isolator is in tension-compression mode as shown in Figure 20, the asymmetric hysteresis curves are observed as shown in Figure 21.

Asymmetric hysteresis loop with hardening overlapping loading envelope are modelled by the followings,

$$F_r(t) = F_{2a}(t)[F_{1a}(t) + z(t)], \tag{3.9}$$

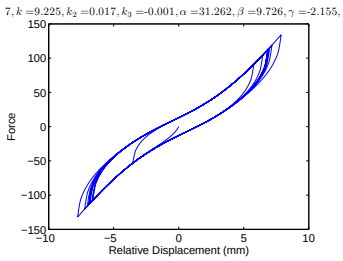

Fig. 19. Hysteresis curves for soft-hardening Bouc-Wen Model

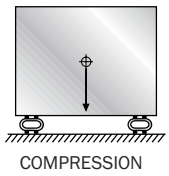

Fig. 20. The tension-compression mode of helical isolator

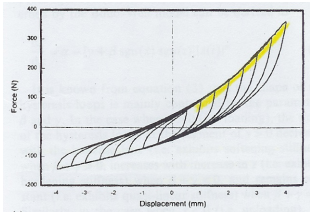

Fig. 21. The Asymmetric hysteretic behavior in tension-compression mode

where

$$F_{1a} = k_1 x(t) + k_2 \ \mathrm{sgn}(x) x^2(t) + k_3 x^3(t), \tag{3.10}$$

$$F_{2a} = k^{cx(t)}. \tag{3.11}$$

Example 3.3: In this example we consider a hysteresis loop in tension-compression mode which is under cyclic loading. For illustration purpose, the related parameters are chosen as:

$$k = 1.799, c = 0.202, k_1 = 39.145, k_2 = 1.360, k_3 = 0.156,$$
$$n = 0.434, \alpha = 147.761, \beta = 44.726, \gamma = -15.512.$$

The corresponding hysteresis loops are given in Figure 22.

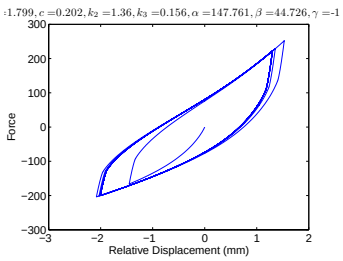

Fig. 22. Asymmetric Hysteresis loops for tension-compression mode

IV. Conclusions

In this paper we briefly review the characteristics of the wire rope isolators, which have been widely used in shock and vibration isolation. The most important one is the hysteresis behavior. Two types of mathematical models that had been proposed to predict this renowned phenomenon, namely Tinker and Bouc-Wen model. From the simulation results, it is observed that for the helical type wire rope isolator, Bouc-Wen model provides much more flexibility to better predict the soft-hardening and asymmetric hysteresis loops.

Acknowledgements

This research was supported by the Industrial Technology Research Institute through Grant ITRI 3000108944. The authors acknowledge the support of Department of Industrial Technology of the Ministry of Economic Affairs, R.O.C., through "Science Technology" program.

References

[1] M. L. Tinker, "Modeling of nonlinear vibration isolators using the advanced continuous simulation language (ACSL)," in *SE Simulation Conference Proceedings*, October 1993.

[2] R. C. Wang, A. J. Miscoe, and W. M. McKewan, "Model for the structure of round-strand wire ropes," U.S. DEPARTMENT OF HEALTH AND HUMAN SERVICES, Pittsburgh, PA, Report of Investigation RI 9644, September 1998.

[3] A. M. Veprik, "Vibration protection of critical components of electronic equipment in harsh environmental conditions," *Journal of Sound and Vibration*, vol. 259, no. 1, pp. 161–175, 2003.

[4] R. Iwankiewicz, M. R. Sotera, and L. Tellier, "Analytical solution techniques for different damping models in random vibration problems."

[5] P. M. Sain, M. K. Sain, J. B. F. Spencer, and J. D. Sain, "The Bouc hysteresis model: An initial study of qualitative characteristics," in *Proceedings of the American Control Conference*, Philadelphia, Pennsylvania, U. S. A., June 1998.

[6] Y. Q. Ni, J. M. Ko., C. W. Wong, and S. Zhan, "Modelling and identification of a wire-cable vibration isolator via cyclic loading test. part 1: experiments and model development," *Journal of Systems and Control Engineering, IMechE*, vol. 213, no. 3, pp. 163–171, 1999.

[7] Y. Q. Ni, J. M. Ko, and C. W. Wong, "Nonparametric identification of nonlinear hysteretic systems," *Journal of Engineering Mechanics*, pp. 206–215, February 1999.